Segregation of Transcription and Replication Sites Into Higher Order Domains

Xiangyun Wei, Jagath Samarabandu,* Rakendu S. Devdhar, Alan J. Siegel, Raj Acharya, Ronald Berezney†

Microscopy shows that individual sites of DNA replication and transcription of mammalian nuclei segregate into sets of roughly 22 and 16 higher order domains, respectively. Each domain set displayed a distinct network-like appearance, including regions of individual domains and interdigitation of domains between the two networks. These data support a dynamic mosaic model for the higher order arrangement of genomic function inside the cell nuclei.

Genomic processes have an underlying structural organization in the cell nucleus (*1, 2*). The genome itself is arranged into discrete chromosome-specific territories (*3*), and there is an emerging view that the genome and its associated functional domains are dynamically linked in an overall nuclear architecture termed the nuclear matrix (*1, 2, 4*). Numerous studies have demonstrated that the sites of DNA replication, transcription, RNA splicing factors, and RNA tracks visualized in the nucleus of the intact cell are spatially maintained following extraction for nuclear matrix (*5–7*).

Another approach to investigating the relationship of nuclear architecture to genomic function is to determine whether the individual sites of replication or transcription, or both, are arranged into higher order domains in the cell nucleus. We directly addressed this issue by simultaneously labeling sites of replication and transcription in permeabilized mouse 3T3 or human diploid NHF1 fibroblasts (*8*). Fluorescence laser scanning confocal microscopy and three-dimensional image analysis were then used to visualize the individual sites of replication and transcription, and the spatial relationships between these sites (*9*). The extranucleolar transcription sites that are visualized with this procedure are predominantly, if not exclusively, transcribed by RNA polymerase II (*8*).

We found that the individual sites of DNA replication and transcription are spatially distinct (separate red and green colors) during all periods of the S phase (Fig. 1) (*10*). More than 95% of the replication sites activated early in the S phase do not coincide with transcription sites (*11*). A yellow color represents an overlap between red and green signals. The very small percentage of yellow sites observed (arrows in Fig. 1I) is likely due to the occasional overlay of the green replication and red transcription sites at different levels in three-dimensional space, rather than concurrence of red and green fluorescence at a single site. We routinely observe this phenomenon in optical sections of mixed red and green fluorescence beads. These results are consistent with those of Wansink *et al.* (*12*) but in direct contradiction to those of Hassan *et al.* (*13*).

We observed that replication (thin arrows; Fig. 1F) and transcription sites (thick arrows; Fig. 1F), aside from being separate from one another, were grouped into separate and distinct clusters. To study the overall distribution of individual sites, we performed contour analysis on individual optical sections at mid-plane (Fig. 2, A and B) in nuclei showing typical early S phase replication patterns (*14*). Of the contoured area in the extranucleolar regions (*15*),

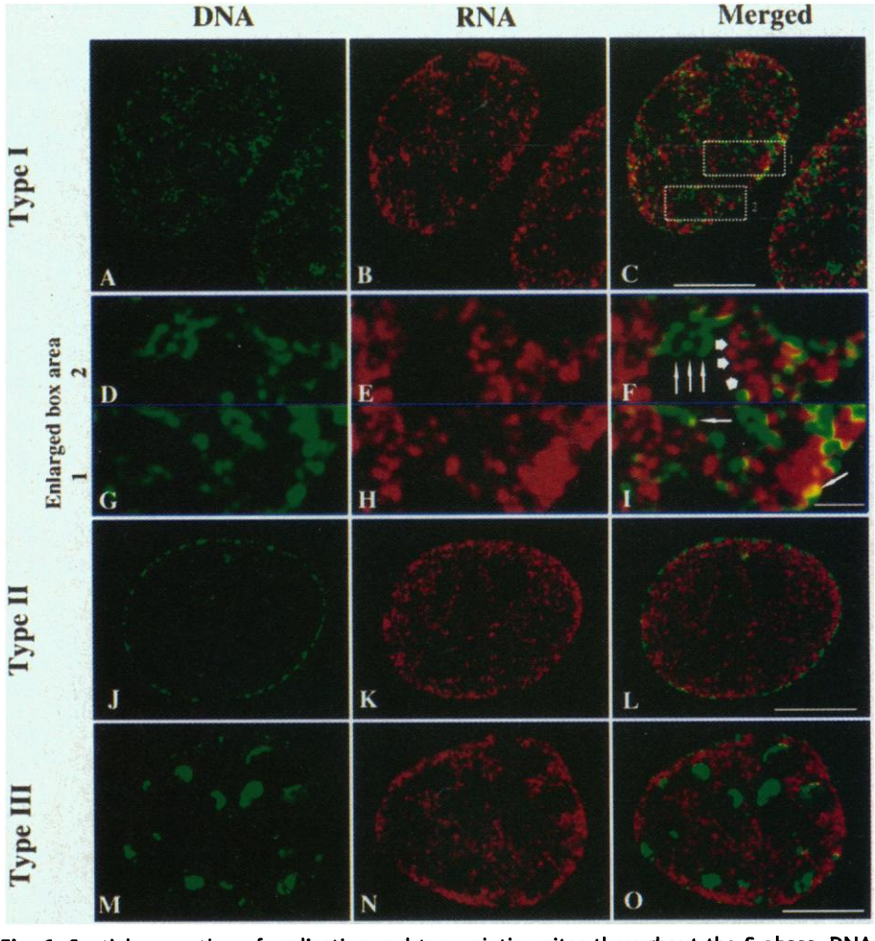

Fig. 1. Spatial separation of replication and transcription sites throughout the S phase. DNA replication and transcription sites are visualized in green and red, respectively, in mouse 3T3 cells. Merged images of replication and transcription sites are displayed in the right panels. (**A** through **I**) Early S phase. Enlarged areas are displayed in (D) through (I). (F) Thick and thin arrows indicate clusters of transcription and replication sites, respectively. Examples of apparent overlap between transcription and replication sites are indicated with arrows in (I). (**J** through **L**) Middle to late S phase. (**M** through **O**) Late S phase.

X. Wei, J. Samarabandu, A. J. Siegel, R. Berezney, Departments of Biological Sciences, State University of New York at Buffalo, Buffalo, NY 14260, USA. R. S. Devdhar and R. Acharya, Department of Electrical and Computer Engineering, State University of New York at Buffalo, Buffalo, NY 14260, USA.

*Present address: Life Imaging Systems, 195 Dufferin Avenue, Suite 300, London, Ontario N6A1K7, Canada. †To whom correspondence should be addressed. E-mail: berezney@acsu.buffalo.edu

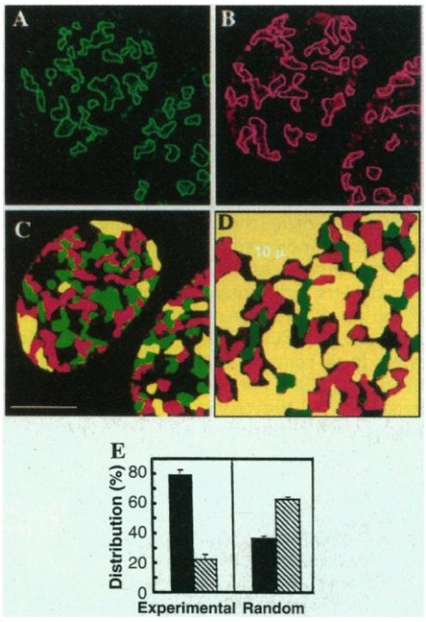

Fig. 2. Preferential clustering of replication and transcription sites in early S phase. (**A**) Clustered replication sites are contoured with light green lines. (**B**) Clustered transcription sites are contoured with pink lines. (**C**) Areas occupied by replication site clusters and transcription site clusters are filled with green and red, respectively. Areas occupied with replication and transcription sites in a mixed pattern are filled with yellow. Nuclear areas with sparsely distributed replication and transcription sites are not contoured and appear as black regions (*14*). (**D**) The same contour analysis was applied to a computer-generated random sampling model (*17*). (**E**) Bar plot of percentage distribution of separate clustered (black bars) versus mixed (striped bars) areas in the extranucleolar regions of experimental samples and random sampling (*16*). Error bars denote the standard error of the mean.

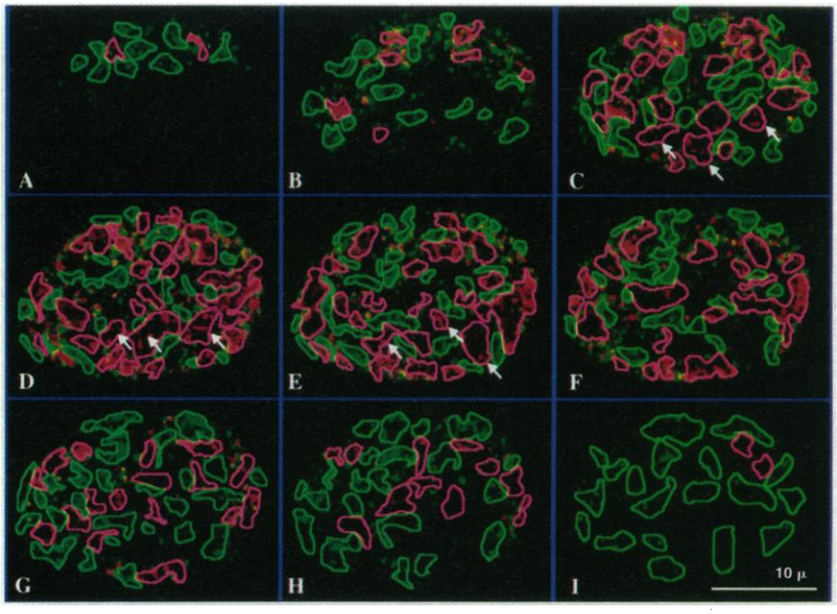

Fig. 3. Cluster distribution of replication and transcription sites in early S phase extending into several optical sections. To study the cluster distribution in three dimensions, the same contour analysis was applied to a series of optical sections (**A** through **I**) of mouse fibroblast nuclei labeled for replication (light green contours) and transcription (pink contours) sites. Three nucleolar transcription clusters are also contoured in pink (indicated with arrows).

77.4% were occupied by separate clusters of replication and transcription sites (Fig. 2, C and E). Because this analysis was performed on exponentially dividing cells, the findings should reflect the entire early S period (approximately 4 hours), when most active genes are replicated (*10*). Similar results were obtained in cells labeled immediately after release from the G_1/S border (*16*). This indicates preferential grouping, because only 36.9% of the extranucleolar area is predicted to form separate replication and transcription clusters by a random clustering model (Fig. 2, D and E) (*17*).

We next examined the replication and transcription clusters in three dimensions. Contour analysis was performed on individual optical sections for each nucleus (Fig. 3) followed by three-dimensional reconstruction (Fig. 4) (*18*). Individual contours corresponding to specific clusters of replication (Fig. 4A) or transcription (Fig. 4C) sites typically extended into several optical sections (0.5 μm per section). An average of 22 ± 2.7 and 16 ± 1.6 higher order domains for replication and transcription were calculated at a given instant in early S phase. Each set of higher order domains was further arranged into a discontinuous network-like appearance that extended throughout the nuclear volume (Fig. 4, A and C). Small regions of individual domains within each set were often found in close apposition with neighboring domains (Fig. 4, A through D). Although the network patterns corresponding to each set of domains appeared similar, they occupied completely separate regions of the nuclear volume (Fig. 4E). Individual domains from corresponding sets, however, were strongly juxtaposed throughout the overall three-dimensional arrangement (Fig. 4).

Previous studies indicate that individual sites of replication and transcription in the cell nucleus are composed of numerous replicons and genes, respectively (*5, 6*). Our results demonstrate an even higher order arrangement of these genomic sites. The extranucleolar region of the nucleus is segmented into a mosaic of spatially juxtaposed replication and transcription domains. Each individual domain contains numerous individual sites of replication or transcription, which are under common temporal control.

We propose that different domains of replication and transcription are progressively activated and inactivated as the cell transverses the S phase and that the changing spatial patterns of these higher order domains correlate with temporal programs of replication and transcription in the cell. In this way, a domain may function in replication at one time and in transcription at another time in S phase. Studies of replication timing of specific gene sequences provide further support for this conclusion (*10*). The interdigitation of replication and transcription domains that we observed in three dimensions may, therefore, be an indication of dynamic cross-talk between the replication and transcription domains or temporal transitions from one functional state to the other.

Arrangement of separate replication and transcription domains into even higher order network patterns suggests an underlying architectural basis. The notable preservation of replication and transcription sites on the nuclear matrix following in situ extraction (*5, 6*) implicates a dynamic nuclear architecture as a basis for these global spatial properties of genomic function. The recent identification of a specific nuclear matrix targeting sequence provides a possible direct approach for further study of higher order functional domains and nuclear architecture (*19*).

References and Notes

1. R. Berezney and K. W. Jeon, Eds., *Structural and Functional Organization of the Nuclear Matrix* [previously published in *Int. Rev. Cytol.*, vols. 162, A and B (Academic Press, New York, 1995)].
2. D. L. Spector, *Annu. Rev. Cell Biol.* **9**, 265 (1993); Y. Xing, C. V. Johnson, P. R. Dobner, J. B. Lawrence, *Science* **259**, 1326 (1993); M. Hoffman, *ibid.*, p. 1257; Y. Baskin, *ibid.* **268**, 1564 (1995).

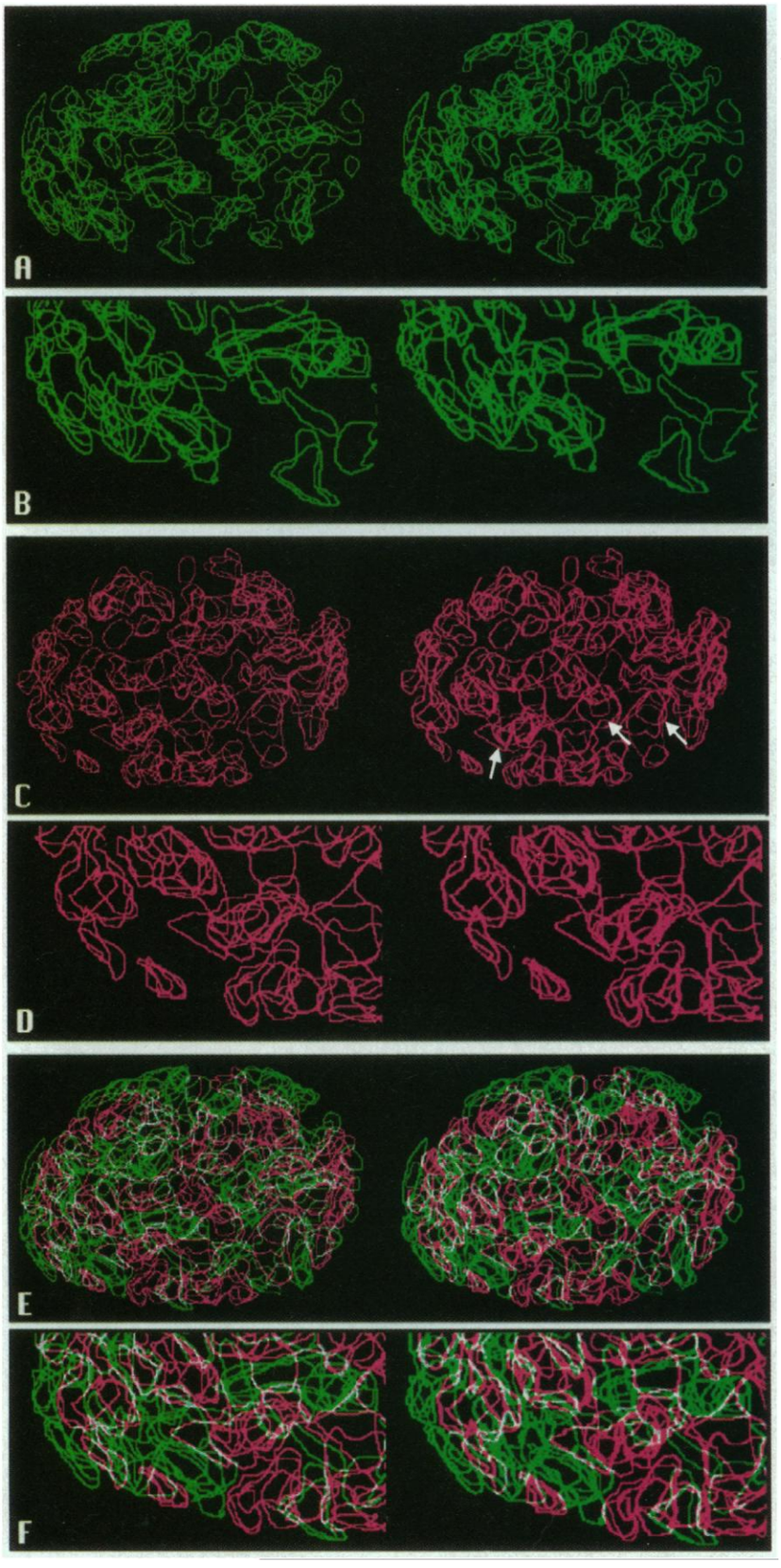

Fig. 4. Replication and transcription sites in early S phase separate into distinct higher order domains in three dimensions. Replication and transcription site clusters drawn on individual optical sections were reconstructed to visualize the spatial relationship of clusters between different sections. In this particular mouse fibroblast nucleus, three-dimensional observation shows that replication site clusters form 24 higher order domains, and transcription site clusters form 20 higher order domains, three of which are located in nucleolar regions (indicated with arrows). **(A)** Stereopair of three-dimensional reconstructed DNA replication site clusters (light green contours). **(B)** Enlargement of the lower left part of (A). **(C)** Stereopair of three-dimensional reconstructed RNA transcription site clusters (pink contours). **(D)** Enlargement of the lower left part of (C). **(E)** Stereopair of merged image. **(F)** Enlargement of the lower left part of (E). All stereoimages were constructed with a 10° angle.

3. S. M. Stack, D. B. Brown, W. C. Dewey, *J. Cell Sci.* **26**, 281 (1977); T. Cremer *et al.*, *Cold Spring Harbor Symp. Quant. Biol.* **58**, 777 (1993).
4. R. Berezney, in *Chromosomal Non-Histone Proteins*, L. S. Hnilica, Ed. (CRC Press, Boca Raton, FL, 1984), vol. 4, pp. 119–180.
5. H. Nakayasu and R. Berezney, *J. Cell Biol.* **108**, 1 (1989).
6. D. A. Jackson, A. B. Hassan, R. J. Errington, P. R. Cook, *EMBO J.* **12**, 1059 (1993).
7. H. C. Smith, R. L. Ochs, E. A. Fernandez, D. L. Spector, *Mol. Cell. Biochem.* **70**, 151 (1986); Y. Xing and J. B. Lawrence, *J. Cell Biol.* **112**, 1055 (1991).
8. Labeling of DNA and RNA synthesis sites, which was performed based on previously published methods and drug inhibition experiments, indicates that extranucleolar transcription sites visualized with this procedure are predominantly, if not exclusively, mediated by RNA polymerase II [(*5, 6*); D. G. Wansink *et al.*, *J. Cell Biol.* **122**, 283 (1993)]. Cells permeabilized with 0.025% Triton X-100 were immediately incubated with nuclei acid synthesis buffer [50 mM tris-HCl (pH 7.4), 10 mM $MgCl_2$, 150 mM NaCl, 25% glycerol, 0.5 mM phenylmethylsulfonyl fluoride, RNasin (25 U/ml), 1.8 mM ATP, 0.5 mM CTP, GTP, BrUTP, 0.1 mM dATP, 0.1 mM dCTP, 0.1 mM dGTP, and 25 μM digoxigenin-11-dUTP] at room temperature for 30 min to label transcription sites and replication sites simultaneously, then were fixed in 100% methanol at –20°C for 20 min followed by 3% paraformaldehyde in phosphate-buffered saline on ice for 5 min.
9. For labeling RNA sites, rat monoclonal antibody to BrdU (Sera-Lab) was used followed by biotin-conjugated goat anti-rat immunoglobulin G and Texas red–conjugated stepavidin incubation. Fluorescein isothiocyanate (FITC)–conjugated sheep anti-digoxigenin Fab fragments (Boehringer Mannheim) were used for labeling DNA sites. Images from 0.5-μm optical sections were collected with a Bio-Rad MRC-1024 confocal microscope equipped with a krypton argon laser to excite FITC and Texas red simultaneously at 488-nm and 568-nm wavelength, respectively.
10. DNA replication is temporally controlled in the S phase, with transcriptionally active genes usually replicated in early S phase and nonactive genes in late S phase [M. A. Goldman, G. P. Holmquist, M. C. Gray, L. A. Caston, A. Nag, *Science* **224**, 686 (1984); K. A. Hatton *et al.*, *Mol. Cell. Biol.* **8**, 2149 (1988); S. Selig, K. Okumura, D. C. Ward, H. Cedar, *EMBO J.* **11**, 1217 (1992)]. Also, DNA replication sites show different patterns in different periods of S phase (*5*).
11. Visual comparison of replication sites and transcription sites was used to determine the number of replication sites that are colocalized with transcription sites. The total numbers of replication and transcription sites were calculated, using a segmentation algorithm specifically developed in our laboratory for three-dimensional confocal images [J. Samarabandu, H. Ma, R. Acharya, P. C. Cheng, R. Berezney, *Proc. SPIE* **2434**, 370 (1995)].
12. D. G. Wansink *et al.*, *J. Cell Sci.* **107**, 1449 (1994).
13. A. B. Hassan, R. Errington, N. White, D. Jackson, P. Cook, *J. Cell Sci.* **107**, 425 (1994).
14. Using Microsoft Power Point, nuclear regions with three or more sites of one and only one activity were contoured as preferential cluster regions. Regions with mixed distribution patterns of replication and

transcription sites were displayed as yellow. The relative sizes of the corresponding areas were directly measured.
15. If we include nucleolar regions in the transcription cluster category, the area occupied by clustered replication and transcription sites will increase to about 80% of the total contoured areas.
16. Synchronization was achieved by serum deprivation followed by aphidicolin inhibition at the G_1/S border [S. Spadari *et al.*, *Drug Res.* **35**, 1108 (1985)]. Contour analysis on 3T3 mouse cells synchronized at the G_1/S border showed that 64% of the contoured area is occupied by replication and transcription site clusters.
17. Cluster analysis was performed on "Sn" number of clusters that were generated using the "random ( )" library function. Of the total number of sites, some were randomly chosen to be transcription sites (red) and the remaining were marked as replication sites (green). Computation of radii of clusters is based on a Gaussian distribution function with a standard deviation of 1.7.
18. Three-dimensional reconstruction of the contours was performed from the confocal optical sections using the drawing tool of IPlab (Signal Analytics).
19. C. Zeng *et al.*, *Proc. Natl. Acad. Sci. U.S.A.* **94**, 6746 (1997); C. Zeng *et al.*, *ibid.* **95**, 1585 (1998).
20. R. Summers and A. Stonebraker (Confocal Microscopy and 3D Imaging Facility of the School of Medicine and Biomedical Sciences, SUNY at Buffalo) provided valuable assistance with confocal microscopy. Computer image analysis was performed at the Microscopic Imaging Facility (Department of Biological Sciences, SUNY at Buffalo). NHF-*1* normal human fibroblast cells were kindly provided by D. G. Kaufman, University of North Carolina, School of Medicine. Supported by NIH grant GM 23922 (R.B.) and a Mark Diamond Graduate Student Research Grant from SUNY at Buffalo (X.W.) (45F97).

20 April 1998; accepted 17 July 1998

CBP: A Signal-Regulated Transcriptional Coactivator Controlled by Nuclear Calcium and CaM Kinase IV

Sangeeta Chawla,* Giles E. Hardingham,* David R. Quinn,† Hilmar Bading‡

Recruitment of the coactivator, CREB binding protein (CBP), by signal-regulated transcription factors, such as CREB [adenosine 3′,5′-monophosphate (cAMP) response element binding protein], is critical for stimulation of gene expression. The mouse pituitary cell line AtT20 was used to show that the CBP recruitment step (CREB phosphorylation on serine-133) can be uncoupled from CREB/CBP–activated transcription. CBP was found to contain a signal-regulated transcriptional activation domain that is controlled by nuclear calcium and calcium/calmodulin–dependent (CaM) protein kinase IV and by cAMP. Cytoplasmic calcium signals that stimulate the Ras mitogen–activated protein kinase signaling cascade or expression of the activated form of Ras provided the CBP recruitment signal but did not increase CBP activity and failed to activate CREB- and CBP-mediated transcription. These results identify CBP as a signal-regulated transcriptional coactivator and define a regulatory role for nuclear calcium and cAMP in CBP-dependent gene expression.

The coactivator CBP and its close relative p300 are vital components of the cellular machinery that regulate gene expression (*1, 2*). CBP can connect sequence-specific transcriptional activators to components of the basal transcription machinery (*3, 4*) and may disrupt repressive chromatin structures through its intrinsic or associated histone acetyltransferase activity (*5*). Signals from the environment are thought to induce gene transcription by activating intracellular biochemical pathways that control the ability of transcription factors to recruit CBP to specific promoters (*3, 6–8*). In this study, we investigated the possibility that intracellular signaling mechanisms, in addition to leading to CBP recruitment, control the rate of gene transcription by regulating CBP activity. CREB phosphorylated on Ser^{133} is the prototypical CBP-interacting transcriptional activator (*1*). Using the mouse pituitary cell line AtT20, we first assessed phosphorylation of CREB on Ser^{133}, the CBP recruitment signal (*1–3, 9*), in immunocytochemical experiments with an antibody specific for CREB phosphorylated on Ser^{133} (*10*). CREB-mediated transcriptional responses were analyzed in parallel with an expression vector encoding GAL4-CREB, which was microinjected together with the reporter gene pF222ΔCREmyc. This construct contains the human c-*fos* gene including 222 base pairs (bp) of upstream regulatory sequence. It lacks the c-*fos* CRE (ΔCRE) and contains a single GAL4 site, which, upon binding of GAL4-CREB, can confer calcium (Ca^{2+}) inducibility to the reporter gene (*11*). A Myc epitope was inserted in frame into the fourth exon of the c-*fos* gene, allowing expression of the reporter gene to be detected at the single cell level by immunofluorescence with the 9E10 antibody and to be quantified by confocal laser scanning microscopy (*11*). Entry of Ca^{2+} into AtT20 cells, a mouse pituitary cell line, through L-type Ca^{2+} channels [triggered by KCl-induced membrane depolarization in the presence of the L-type Ca^{2+} channel agonist FPL 64176 (KCl-FPL treatment)] (*11*) induced phosphorylation of CREB on Ser^{133} followed by CREB-mediated transcriptional activation (Fig. 1A).

Because Ca^{2+} acts in two cellular compartments, the nucleus and the cytoplasm, to activate gene expression by distinct mechanisms (*11*), we analyzed the control of CREB phosphorylation on Ser^{133} by spatially distinct Ca^{2+} signals. Selective inhibition of nuclear Ca^{2+} transients by means of nuclear microinjection of a nondiffusible Ca^{2+} chelator, BAPTA-D70 [1,2-bis(2-aminophenoxy)ethane-*N,N,N′,N′*-tetraacetic acid linked to a 70-kD dextran molecule] (*11*), blocked CREB-mediated transcription in response to KCl-FPL but had little inhibitory effect on CREB phosphorylation on Ser^{133} (Fig. 1A). Thus, nuclear and cytoplasmic Ca^{2+} signals have distinct roles in CREB regulation. Activation of cytoplasmic Ca^{2+} signaling pathways stimulates CREB phosphorylation on Ser^{133} but, in the absence of nuclear Ca^{2+}, CREB remains transcriptionally inactive. A second regulatory event is apparently triggered by nuclear Ca^{2+} and leads to transcriptional activation. CREB contains another phosphorylation site, Ser^{142}, that inhibits transcriptional activation by CREB (*12*). However, nuclear Ca^{2+} appears not to control CREB through phosphorylation on Ser^{142} because inhibition of nuclear Ca^{2+} signals also blocked transcriptional activation by a mutant CREB protein, GAL4-CREB(Ser^{142}Ala), which contains a serine-to-alanine mutation at position 142 (*12*).

Ca^{2+}/calmodulin-dependent (CaM) protein kinases are prime candidates for mediating Ca^{2+}-regulated gene expression (*13–15*). Inhibition of CaM kinases with KN-62 did not reduce Ca^{2+}-induced CREB phosphorylation on Ser^{133} (Fig. 1B) but did inhibit CREB-mediated transcriptional ac-

Medical Research Council, Laboratory of Molecular Biology, Hills Road, Cambridge CB2 2QH, UK.

*These authors contributed equally to this work.
†Present address: Department of Clinical Biochemistry, University of Cambridge, Addenbrooke's Hospital, Hills Road, Cambridge CB2 2QR, UK.
‡To whom correspondence should be addressed. E-mail: hb1@mrc-lmb.cam.ac.uk